Influence of poly(ε-caprolactone) end-groups on the temperature-induced macroscopic gelation of Pluronic in aqueous media

Natalie Gjerde[a]

Kaizheng Zhu[a]

Kenneth D. Knudsen[b, *]

Kenneth.knudsen@ife.no

Bo Nyström[a, *]

bo.nystrom@kjemi.uio.no

[a]Department of Chemistry, University of Oslo, P.O. Box 1033, Blindern, N-0315 Oslo, Norway

[b]Department of Physics, Institute for Energy Technology, P. O. Box 40, N-2027 Kjeller, Norway

*Corresponding authors.

Abstract

Temperature-induced gelation of amphiphilic copolymers in aqueous media has attracted a great deal of interest in recent years. We have investigated phase behavior, gelation, rheology, and structure of modified versions of the water-soluble copolymer of type PEO-PPO-PEO (Pluronic, F127) with short (PCL(5)) or long (PCL(11)) poly(caprolactone) blocks at both ends. By visual inspection of the studied semidilute and concentrated polymer samples at various temperatures, gelation and phase separation could be mapped and the length of the PCL blocks had a strong impact on the observed features. By using oscillatory shear experiments, the gel points of the systems were determined and an interesting anomaly of the complex viscosity was observed at high frequencies where the moieties were kinetically arrested. This irregularity was strengthened for the PCL(11) copolymer and this was ascribed to bridging of the micelles due to the long PCL blocks. The mesoscopic structure of the systems was studied by using small angle neutron scattering. The position and amplitude of the observed correlation peak, which discloses vital intermicellar correlations in the scattering function depends on temperature, concentration, and the length of the PCL blocks. Frequently the scattering function could be portrayed by a spherical core-shell micelle model with hard sphere interaction between them. The estimated aggregation number (N_{agg}) was substantially affected by the PCL content of the polymer and a significant influence of polymer concentration and temperature on the value of N_{agg} was found.

Keywords: PCL-modified Pluronic; Rheology; SANS; Complex viscosity anomaly; Aggregation number

1 Introduction

In recent years it has been established that amphiphilic block copolymers with different architectures and chemical composition that self-assemble and form hydrogels in the semidilute concentration regime in response to external stimuli, are an essential class of soft materials with applications in areas such as drug delivery, gene delivery, tissue engineering, and smart surface coatings [1–10]. For instance, decades of experimental and theoretical studies have established a solid background for gaining insight into self-assembling, micelle and gel formation, structures, and phase behavior of Pluronic triblock copolymers, which are one of the most studied commercially available amphiphilic copolymers, composed of hydrophilic poly(ethylene oxide) (PEO) at both ends and a hydrophobic poly(propylene oxide) block as a spacer [11–15]. However, because of the rather low hydrophobicity of the PPO-block in Pluronics it has been pointed out [16,17] that this type of copolymer is not suitable as a long-term drug delivery vehicle since it has short gel duration (less than 1 day) after implanting the hydrogel in the subcutaneous layer. To strengthen the hydrophobicity and to be able to design a durable and degradable thermogel, it is possible to equip Pluronic with hydrophobic poly(ε-caprolactone) (PCL) groups. In a recent study [18], we synthesized modified versions of the copolymer of the type PEO-PPO-PEO (Pluronic, F127) with short poly(ε-caprolactone) (PCL(5)) or long (PCL(11)) PCL blocks at both ends. We reported how temperature and length of the PCL end-groups affect the self-assembling of the copolymer in dilute aqueous solution. By employing a variety of experimental methods, it was possible to map-out an intricate interplay between unimers, micelles, and clusters and the size, size distribution, and structure of the species were determined. The small angle neutron scattering (SANS) results at different temperatures, disclosed some major structural changes from spherical core-shell to cylindrical core-shell architectures and the appearance of pronounced correlation peaks in the SANS data suggested salient intermicellar interactions.

In view of these findings, we decided to investigate what kind of structures and rheological behavior appear in the semidilute concentration regime and in the hydrogels formed at elevated temperatures. An essential issue is how the features are affected by the incorporation of PCL-blocks of different lengths at both ends of F127. To accomplish this task, we have carried out rheology and SANS experiments, complemented with gel phase separation studies. The aim of this work is to understand the impact of the PCL end-groups in the formation of the transient network in the semidilute concentration range and how the gel-formation evolved at higher temperatures will be affected by the PCL-groups. This study on semidilute systems will reveal that the PCL modification of Pluronic leads to significant alterations of the rheological features, as well as consequences on the local structure probed by SANS.

2 Experimental

2.1 Materials

The PCL end-groups were prepared from ε-caprolactone (CL) that was obtained from Sigma-Aldrich and CL was dried and distilled over CaH_2 under reduced pressure and stored in a refrigerator. The Pluronic triblock copolymer denoted F127 was purchased from Aldrich and was used after drying under vacuum at 90 °C for 24 h. The catalyst used in the polymerization was stannous 2-ethylhexanoate (stannous octoate, $Sn(Oct)_2$) and it was purchased from Sigma-Aldrich and used without further purification. The other chemicals that were employed were of reagent grade and were not purified further.

2.2 Synthesis of the block copolymers

For this study, modified Pluronic (F127) derivatives were synthesized employing ring opening polymerization (ROP) to attach poly(ε-caprolactone) at both ends of the Pluronic chain, yielding $P(CL)_n$-F127-$P(CL)_n$, with two analogs (n = 5 and n = 11). To simplify the notation of the copolymers, we will call the unmodified Pluronic F127 and the PCL-modified copolymers with n = 5 and n = 11 for PCL(5) and PCL(11), respectively, through the rest of the paper. In this ROP process, Pluronic acts as the macroinitiator and stannous octoate is the catalyst. PCL is a semi-crystalline polymer with a strong hydrophobic character that makes this compound stable over long times in aqueous environment. A detailed description of the synthesis and characterization of the $P(CL)_n$-F127-$P(CL)_n$ compounds have been reported previously [18].

2.3 Construction of phase diagrams

The phase diagrams for the three copolymer systems were constructed by using the inverted tube method [19]. For each polymer sample several concentrations were prepared to map gelation and phase separation. For the copolymer with the longest PCL-end groups, concentrations higher than about 10 wt% could not be used because of solubility problems. 1 ml of the solutions was transferred into small tubes and they were kept in a water bath and heated slowly from 5 to 85 °C. At temperatures close to phase separation and/or gelation the samples were allowed to equilibrate at that temperature for 10 min. The sol-gel transition temperature was determined by a flow to non-flow criterion over 1 min. The reproducibility was checked by heating a second bath of prepared samples.

2.4 Rheological measurements

Oscillatory shear experiments were carried out with an Anton Par-Physica MCR 301 rheometer by employing the cone-plate geometry with a diameter of 75 mm and a cone angle of 1°, or a cone with 25 mm diameter and a cone angle of 4°. The smaller cone-plate system was used for samples of high concentrations to reduce the amount of sample needed. It was always checked that the results were not affected by the type of cone-plate system. The instrument is equipped with a Peltier plate, providing an effective temperature control (±0.05 °C) for an extended time over the studied temperature region. To avoid dehydration of the samples at elevated temperatures and extended times, a low-viscosity silicone oil was applied on the free surface of the solutions. The low-viscosity oil does not affect the viscoelastic response of the sample. The rheometer was calibrated with water and standard high-viscosity oil before performing any experiment. The appropriate amplitude sweep for the experiments was chosen to ensure that the measurements were conducted in the linear viscoelastic region, where the dynamic storage modulus (G′) and loss modulus (G″) are independent of the strain amplitude. The angular frequency (ω) was varied from 0.1 to 100 rad s^{-1}, with a constant strain of 0.1%. At every temperature, the samples were allowed to equilibrate for 20 min. To check the reproducibility, new samples were tested for every concentration.

The evolution of the rheological properties during gelation and in the post-gel region can be monitored through the complex viscosity, with its absolute value $|\eta^*(\omega)|$ given by [20].

$$\left|\eta^*(\omega)\right| = ((G')^2 + (G'')^2)^{1/2}/\omega \quad \textbf{(1)}$$

The frequency dependence of the absolute value of the complex viscosity for an incipient gel can be described in terms of a power law [21]. $|\eta^*(\omega)| \propto \omega^{-m}$, where the complex viscosity exponent m is directly related to the frequency dependence of the dynamic moduli ($G' \propto G'' \propto \omega^n$) at the gel point through m = 1 − n. Values of m close to zero announce liquid-like behavior, whereas values of m approaching 1 suggest solid-like response of the system.

2.5 Small angle neutron scattering experiments

The SANS experiments were carried out at selected temperatures in the range from 10 to 70 °C with the SANS installation at the JEEP II reactor at IFE, Kjeller, Norway. At each temperature the sample was equilibrated for 2 h.

The neutron detector was a 128×128 pixel, ^{3}He filled RISØ-type, mounted on rails inside an evacuated detector chamber. The distance varied from 1.0 to 3.4 m and the wavelength was 5.1 Å, giving a wave-vector range from 0.01 to 0.32 $Å^{-1}$. Here q, the absolute value of the wave-vector, is given by $q = (4\pi/\lambda) \sin(\theta/2)$, where θ is the scattering angle and λ is the neutron wavelength. The polymer solutions were held in 2 mm quartz cuvettes, equipped with stoppers. The measuring cells were placed onto a copper base for good thermal contact and mounted in the sample chamber.

The transmission was measured separately, and the absolute scattering cross section (cm^{-1}) was calculated by taking into account the contribution from empty cell and general background. The samples were prepared in heavy water instead of light water to enhance contrast and reduce incoherent background.

The SANS results were analyzed by fitting the data with a spherical core-shell model: the following function was employed to express the form factor within the SASview programming environment [22].

$$P(q) = \frac{\text{scale}}{V_s} F^2(q) + \text{background} \quad (2)$$

$$F^2(q) = \frac{3}{V_s}\left[V_c(\rho_c - \rho_s)\frac{\sin(qr_c) - qr_c\cos(qr_c)}{(qr_c)^3} + V_s(\rho_s - \rho_{solv})\frac{\sin(qr_s) - qr_s\cos(qr_s)}{(qr_s)^3}\right] \quad (3)$$

here V_s is the volume of the whole particle, V_c is the volume of the core, $r_s = \text{radius} + \text{thickness}$ is the radius of the whole particle, r_c is the radius of the core, ρ_c is the scattering length density of the core, ρ_s is the scattering length density of the shell, and ρ_{solv}, is the scattering length density of the solvent.

At conditions of concentration and temperature where micelles are not developed, the unimers are portrayed as linear polymer chains with Gaussian statistics and the formfactor can be expressed by the Debye function representing a Gaussian chain [23].

$$D(x) = 2(e^{-x} + x - 1)/x^2 \quad (4)$$

where $x = (qR_g)^2$ and R_g is the radius of gyration, and this is the only parameter fitted considering that q is given.

For interparticle effects, a hard-sphere interaction model was incorporated for the static structure factor S(q), using the Percus-Yevick closure [22,24]. The interparticle potential is given by,

$$U(r) = \begin{cases} \infty & r < 2R \\ 0 & r \geq 2R \end{cases} \quad (5)$$

where r is the distance from the center of the sphere of a radius R.

For the model fitting of the SANS data, the value for the scattering length density (SLD) of PCL was calculated to 0.85×10^{-6} $Å^{-2}$, and the values used for PEO and PPO were taken from literature [24] as SLD(PEO) = 0.572×10^{-6} $Å^{-2}$ and SLD(PPO) = 0.347×10^{-6} $Å^{-2}$.

3 Results and discussion

3.1 Phase diagrams and gelation

Before we discuss the details of the phase diagrams and sol-to-gel transitions, it may be instructive to give some general comments about the mechanism for temperature-induced gelation of hydrogels. A gel-network is formed in the semidilute or concentrated concentration regime, and the gelation is governed by a delicate balance between connectivity and swelling [25]. The connectivity of the gel-network can be provided by physical crosslinks that are generated by interactions such as intermolecular hydrogen bonds, ionic interactions, and hydrophobic microdomains. The swelling may be caused by repulsive electrostatic ionic groups in the network, or may be due to good thermodynamic solvent conditions (hydrophilic groups). For instance, if the connectivity generated through the hydrophobic microdomains is too dominating, macroscopic phase separation takes place. If, on the other hand, the swelling power is strong and the physical crosslinking zones are in deficiency, a transient network is formed but not a gel-network. For the present copolymers in dilute solutions, it has been established [18] that the formation of micelles from unimers and the evolution of intermicellar complexes are controlled by polymer concentration, temperature, and hydrophobicity (from PPO and/or PCL groups) of the polymeric moieties. Higher values of polymer concentration and temperature and augmented hydrophobicity favor the formation of micelles and intermicellar aggregates, and in the semidilute regime the network is created through packing and bridging (could be important for PCL(11) with long blocks) between neighboring micelles. Especially for Pluronic with PCL-groups, the hydrophobic zones creating the network connectivity and a gel at elevated temperatures may at still higher temperatures promote pronounced turbidity of the sample, and eventually a solid-like gel “white gel” [26] may be formed. In the case of F127, it has been argued that gelation is due to close-packing of spherical micelles [13,27–29]. The status of the network (transient or gel-network) will depend on the ratio between hydrophilic groups and hydrophobic groups (PPO and PCL) and temperature. In the light of this discussion, it is interesting to note that in a number of theoretical studies on temperature-responsive gels, the interference between gelation and two-phase separation was recognized [30–32].

The phase diagrams constructed for the three polymer systems are displayed in Fig. 1. In aqueous solutions of F127 a reversible sol-to-gel transition is observed at polymer concentrations above 20 wt%; the transition is located at higher concentrations when the temperature is lowered. No phase separation is detected at the considered conditions of temperature and polymer concentration. At higher polymer concentrations, a situation evolves where the micelles are close packed [13,27–29] and the concentration of PPO-segments and augmented temperature generate the hydrophobic microdomains necessary for the connectivity of the gel-network. Since no macroscopic phase separation was detected, it suggests that the hydrophobic junction zones are not very large. A similar profile of the phase separation curve has been reported previously [33] for F127, and isotropic solution behavior was observed on the left hand-side of the curve; at higher concentrations a cubic phase was claimed. For the PCL(5) system, a similar behavior as for F127 is found at low and moderate temperatures, whereas at high temperatures (70–80 °C) an incipient phase separation is observed for the PCL(5) sample. Due to the enhanced sticking probability of the PCL segments at elevated temperatures, growing aggregates are formed and this leads to augmented turbidity in the solution and finally macroscopic phase separation.

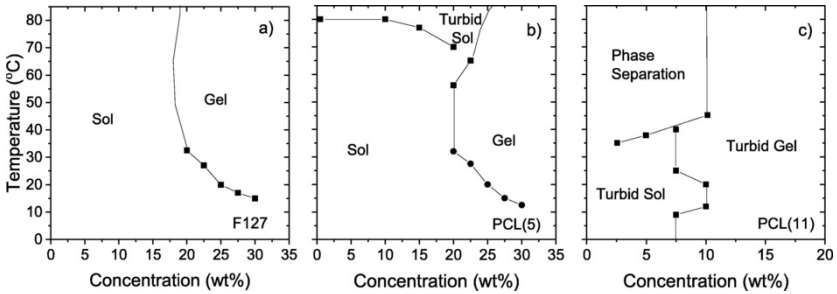

Fig. 1 Phase diagrams for aqueous solutions of (a) F127, (b) PCL(5), and (c) PCL(11). Lines have been added to better illustrate the different phases. See Section 2.2 for an explanation of the copolymer notation.

For the PCL(11) system with longer hydrophobic chains, a more complex picture emerges. In this case it is only possible to dissolve 10 wt% of the polymer in aqueous solution due to the enhanced hydrophobicity generated by the long PCL-groups. Actually, already at concentrations down to 2, 5 wt% the solutions are turbid as confirmed by the previous study [18] on dilute solutions. For this system the sol-to-gel transition is more intricate; it is observed that a 10 wt% solution is transformed to a gel in the refrigerator (ca. 4 °C) and upon gentle heating it turns into a low-viscous solution that is converted into a gel at about 20 °C (see the discussion about the rheological results). A possible explanation is that at low temperatures the connectivity is provided through intermolecular hydrogen bonds and these bonds gradually break as the temperature rises. At 20 °C, the connectivity is again generated by the growth of hydrophobic microdomains, and turbid gels are present at even higher temperatures until macroscopic phase separation takes place. In the liquid phase, macroscopic phase separation occurs at temperatures around 40 °C. For this copolymer with long PCL-ends, elevated temperatures lead to the development of large hydrophobic domains that give rise to phase separation.

3.2 Rheological results

Rheological experiments were conducted to monitor how the viscous and elastic properties of Pluronic in the semidilute concentration regime are affected by the length of the PCL-ends on F127. Temperature dependences of the absolute complex viscosity |η*| for 10 wt% samples (PCL(11) was not soluble at higher temperatures above this concentration) of the three copolymers are depicted in Fig. 2. At this concentration, low viscosity values are observed for F127 and PCL(5) and the data virtually overlap each other, suggesting that the effect of the short PCL-ends has an insignificant impact on the viscosity features. The moderate drop of |η*| with increasing temperature can essentially be ascribed to the temperature dependence of the solvent. For the PCL(11) copolymer, the absolute complex viscosity is significantly higher and the viscosity profile is quite different. Initially, |η*| falls off with rising temperature and this can probably be ascribed to contraction of the hydrophobic domains. The value of |η*| passes a minimum at 19 °C and a strong viscosification occurs at higher temperatures; this is attributed to pronounced hydrophobic associations that reinforce the network, and bridges from the long PCL-chains may also contribute to the strengthening of the network connectivity. The fact that |η*| is almost three decades higher for PCL(11) than the two other copolymers at low temperatures, is a strong indication of that bridging of closely allied micelles plays an important role. Measurements have not been carried out above 30 °C for this copolymer sample because of incipient macroscopic phase separation.

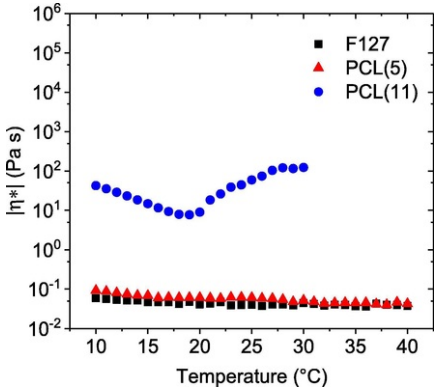

Fig. 2 Temperature dependencies of the complex viscosity for the indicated polymer systems at a polymer concentration of 10 wt% and a fixed angular frequency of 10 rad s^{-1}.

As mentioned, it is not possible to go up to higher concentrations than 10 wt% for the PCL(11) sample, but it is interesting to investigate how the shorter PCL-ends of Pluronic will affect the concentration and temperature dependencies of |η*| (cf. Fig. 3). The most conspicuous feature is the difference in temperature dependence of the complex viscosity for the two copolymers at the lowest concentration (20 wt%). For F127, a marked rise of |η*| is observed at about 17 °C as the gel zone is approached, followed by a plateau region ($|\eta^*| \approx 10^4$ Pas) at temperatures above 30 °C. It is interesting to note that in the case of PCL(5) at 20 wt%, the temperature-induced change of |η*| is much less pronounced with a maximum value of $|\eta^*| \approx 10^2$ Pas; higher temperatures even seem to reduce the value of |η*|. This puzzling effect may be rationalized in the following way. We argue that some of the short PCL-chains may be hidden inside the micelles and higher temperatures leads to contraction of micelles and intermicellar structures. Higher polymer concentration is then needed to restore the network connectivity. At 20 wt% and below, we speculate that only a fragmented network is formed and no full-space spanning connectivity is established.

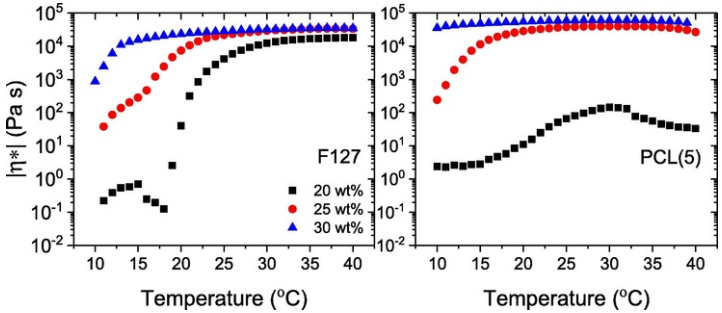

Fig. 3 Temperature dependencies of the absolute complex viscosity for (a) F127 and (b) PCL(5) at the concentrations indicated and at a constant angular frequency of 1 rad s^{-1}.

For the higher two concentrations (25 and 30 wt%), the profiles for the temperature dependence of |η*| are similar for the two copolymers, but the corresponding values of |η*| are higher for PCL(5), which suggests that the PCL groups contribute to the strength of the gel-network. At these concentrations, we have a space-spanning gel-network and the hydrophobic interactions contribute to strengthening the network.

From the frequency dependence of |η*| at various temperatures, it is possible to follow the viscoelastic response of the samples at different stages during the gelation process. This is illustrated in Fig. 4 for the three copolymer samples. The features for the F127 sample are that at early stages (low temperatures) in the pre-gel domain lower values of m ($|\eta^*| \propto \omega^{-m}$) are observed, but the fairly high values ($m \geq 0.8$) suggest viscoelastic behavior that is transformed to a solid-like response (m ≈ 1) at the highest temperature. This type of behavior is similar as reported previously for F127 [34,35]. Most of the considered temperatures are located in the post-gel region for the F127 and PCL(5) systems. By employing the procedure of Winter and Chambon [36], the gel-point during a temperature-induced cross-linking process of a polymer solution can be determined by observation of a frequency-independent value of the loss tangent, tan δ (=G″/G′), obtained from a multifrequency plot of tan δ versus temperature as illustrated in Supporting Information, S1. For the systems F127, PCL(5), and PCL(11), the gel-temperatures are 13 °C (25 wt%), 14 °C (25 wt%), and 21 °C (10 wt%), respectively (see Supporting Information).

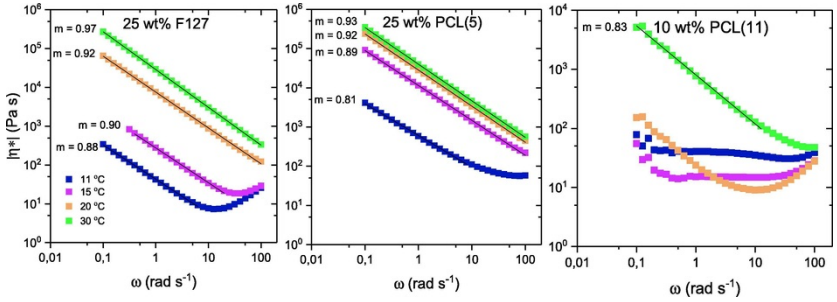

Fig. 4 Frequency sweeps of |η*| from 10 °C to 30 °C for the three copolymers at the concentrations and temperatures indicated.

For the lower two temperatures for the F127 sample, a peculiar increase of |η*| occurs at an angular frequency above 13 rad/s (this corresponds to a characteristic relaxation time $t_c = 2\pi/\omega = 0.48$ s) at 11 °C and at 35 rad/s ($t_c = 0.18$ s) at 15 °C. At higher temperatures (well in the post-gel region), this effect is not visible in the considered frequency range. The anomaly observed at low temperatures may be rationalized in the following scenario. It has been known for a long time that aggregation of colloidal particles experiencing short-range attractive interactions may lead to the emergence of arrested kinetics or jamming at low fractions of colloidal particles because of the evolution of space-spanning structures [37–40]. In this framework, the systems are considered to be jammed if the characteristic relaxation time is longer than the observation window [38], so that the particles appear stuck in a fixed configuration, leading to an augmented complex viscosity as illustrated in Fig. 4. We imagine a scenario where the association network or incipient gel-matrix is disrupted by the oscillatory shear-flow to micellar like entities and at a certain high angular frequency (corresponding to a critical time) they are not able to follow the oscillatory shear-flow. They are then kinetically arrested or jammed and connections are evolved, leading to an enhanced complex viscosity of the sample. Our conjecture is that the transition viscosity is shifted to higher frequencies (lower times) as the temperature is raised, because - with increasing thermal energy of the system - the components of the incipient gel are able to follow the faster perturbations of the oscillatory flow before jamming occurs. After the gel is formed, the arrest has already taken place, so that a transition as observed at lower temperatures is not found. However, one cannot exclude that for temperatures in the post-gel region, this will happen at higher angular frequency values than considered in this study.

When it comes to the structural arrangement of the moieties in connection with the viscosity anomaly, it is possible that the angular frequency gives rise to structural changes. It has been observed [41–43] that oscillatory shear perturbations may induce substantial structural changes such as crystallization.

An incipient effect of this complex viscosity anomaly is also observed for PCL(5) at the lowest temperature; at higher temperatures PCL(5) exhibits similar behavior as F127 (Fig. 4). At higher temperatures, a strong gel-network with high connectivity has emerged and the perturbations are not sufficiently high to break-up the network in separated elements. In the case of PCL(11) (at a concentration of 10 wt%), a more intricate pattern of behavior is evolved for the complex viscosity. For the lower two temperatures, a virtually Newtonian performance of |η*| is found and this indicates that the connectivity of the network has not yet been established. However, at 20 °C (just below the gel point) a conspicuous anomaly in |η*| appears and this can probably be attributed to the jamming effect described above, but in this case it is possible that the self-assembling of the constituents from the network is facilitated through bridging of the moieties through the long PCL chains of the copolymer. At higher temperatures (30 °C), a power-law behavior, similar to that of the other systems, is observed with a value of $m = 0.83$. This indicates that the system approaches solid-like behavior.

3.3 SANS results

To gain information about structural alterations on a mesoscopic dimensional scale, we have carried out SANS experiments on semidilute solutions and gels of F127 and its PCL-modified analogs at various temperatures.

Fig. 5 shows the SANS results for F127 and PCL(5) at two different concentrations (10 and 20 wt%) in the semidilute concentration regime and at temperatures in the range from 10 °C to 70 °C. For the 10 wt% F127 sample (Fig. 5a), the scattered intensity at low temperatures is weakly dependent on q and the absolute intensity is low. The dotted line represents the best fit to the Debye function (see experimental section) under the assumption of Gaussian chains. This yields a radius of gyration of $R_g \approx 1.5$ nm, which has been argued [12] to be too small if the copolymer is fully dissolved and forms Gaussian coils (unimers). It was claimed that the scattered intensity will be dominated by the contribution from the PEO chains that display Gaussian structure, whereas PPO midblock chain segregate into a small condensed core with weak scattering. As the temperature rises, micelles are formed and since the concentration is fairly high (10 wt%) a correlation peak appears as a result of micelle interaction. The peak becomes gradually more pronounced with increasing temperature and the scattered intensity also increases. This peak reveals important spatial correlation between neighboring micelles. Likewise, as the polymer concentration increases (Fig. 5b), the correlation peak becomes more marked and a visible narrowing of the peak is observed with rising temperature; this is a signature of strong micellar ordering and may be related to evolution of a crystalline lattice [12]. In the case of the PCL(5) analog at 10 wt%, we should note some fundamental differences (Fig. 5c). First, due to the enhanced hydrophobicity of this copolymer compared to F127, micelles are formed at all temperatures and no scattering profile indicates unimers. Second, at high temperatures the correlation peak fades away and this suggests that

the spatial ordering of the micelles is lost or a structural change takes place. However, at a concentration of 20 wt% (Fig. 5d) a prominent correlation peak is found with narrowing at higher temperatures and the profiles remind about the corresponding ones from F127, but the total scattered intensity is overall lower. Our hypothesis is that the disappearance of the correlation peak at higher temperatures for the 10 wt% PCL(5) sample can be traced to the formation of a disordered and perhaps fragmented network because of specific hydrophobic interactions. In this case there is no space-spanning network of micelles. However, at a high concentration (20 wt%) the ordering and connectivity of the network is established even at high temperatures due to the large effective volume occupied by the micelles. The effect of temperature on the position of the maximum of the correlation peak will be discussed below.

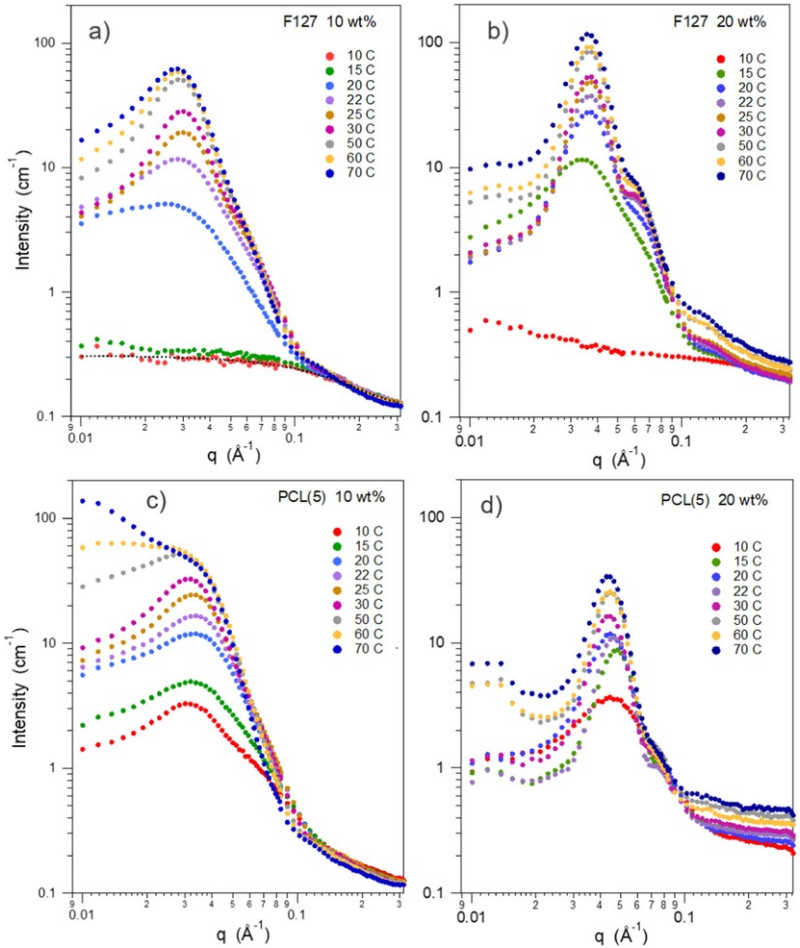

Fig. 5 SANS scattering profiles for F127 and PCL(5) at the concentrations and temperatures indicated. For F127 at 10 °C a model plot corresponding to a Gaussian coil (Debye function) has been included (dotted line).

Temperature dependences of the SANS intensity for 10 wt% samples of PCL(11) at various temperatures are displayed in Fig. 6. In this case the scattering profiles disclose a more complex picture than for the two other copolymers. At temperatures below the gel-point (about 20 °C) the scattering profile is governed by a correlation peak and this peak steadily disappears as the temperature increases. However, at high temperatures (50–70 °C) a noticeable correlation peak appears again. To elucidate the differences in behavior at different temperatures, SANS profiles at some characteristic temperatures are depicted in Fig. 6b. At low temperature (10 °C), below the gel temperature, and at high temperature (70 °C) in the post-gel region, well developed correlation peaks are observed and this feature suggests interacting micelles that are packed with a certain order. Since the correlation peak at 70 °C has a narrower peak positioned at a higher q-value than at 10 °C, the scattering function of the micellar cluster reflects this locally more dense system (cf. the illustration in the inset). The fact that the amplitude of the peak is larger at 70 °C and that the maximum of the peak is shifted to a higher q-value ($d = 2\pi/q_{max}$) can be used to estimate the average intermicellar distance). Hence a smaller average distance between the interacting micelles shows that the number of micelles increases at high temperature. Thus for this hydrophobic sample it appears that instead of increased aggregation number at elevated temperatures, the number of polymer chains inside each micelle are reduced and

continuously more micelles are created. The reason for this behavior can probably be ascribed to the strong hydrophobic contribution for the copolymer with PCL(11) moieties at high temperature; the PCL moieties are likely close-packed inside the micelle to avoid water exposure (strong dehydration) and more micelles are formed due to the augmented sticking probability. The picture that emerges is that at low temperature we have interacting micelles that are packed with a certain order and at high temperature the order is preserved, but the number of micelles has increased and the average distance between them is smaller (cf. the discussion below).

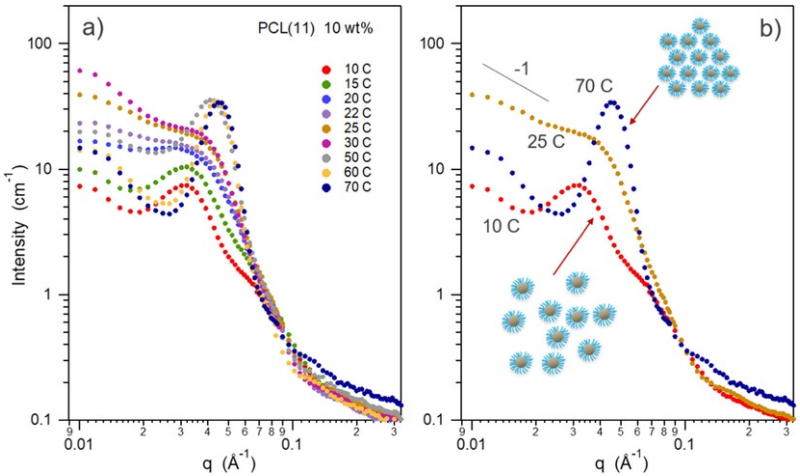

Fig. 6 SANS patterns of PCL(11) versus temperature (from 10 °C to 70 °C) for 10 wt% concentration (a). The panel (b) shows three selected temperatures, and the insets illustrate how a broad correlation peak can result from a partly ordered system (10 °C) and a narrower correlation peak located at higher q-values from a highly ordered system (70 °C) with smaller average micellar distance. This simple schematic does not consider intermicellar aggregates (joining of two or more micelles into an entity) that probably also exists for the PCL(11) sample, given the excess scattering observed at low-q.

The scattering profile for the PCL(11) sample at 25 °C, where an incipient gel has evolved (Fig. 6b), the correlation peak has virtually faded away, indicating that the spatial correlation between neighboring micelles is suppressed. Interestingly, the same type of scattering profile has been observed for incipient gels of a thermoresponsive amphiphilic block copolymers of the type poly(d,l-lactic acid-*co*-glycolic acid)-*block*-poly(ethylene glycol)-*block*-poly(d,l-lactic acid-*co*-glycolic acid) (PLGA-PEG-PLGA) [44]. It was argued that this disorder in structure could be attributed to a loss of the well-defined distance between the micelles as they create a gel-like network. However, this is not a universal feature because a similar type of copolymer poly(ε-caprolactone-co-lactide)-poly(ethylene glycol)-poly(ε-caprolactone *co*-lactide) (PCLA-PEG-PCLA) exhibited a pronounced correlation peak when the incipient gel was formed [45]. It seems that depending on the morphology of the gel network, the substructures may be ordered or disordered in the gel.

At all temperatures in Fig. 6, a noticeable upturn in the scattered intensity was found at low q-values, which suggests the development of large structures. This clearly indicates that substantial structural changes take place, as indicated by the near −1 log-log slope (Fig. 6b) detected at low q. The value of the slope is indicative of locally extended rod-like objects, which may result from micelles that line up in highly asymmetric arrangements.

Effects of polymer concentration on the scattering profiles for the three copolymer systems at a fixed temperature of 30 °C are depicted in Fig. 7a–c. Here we have also included results for dilute systems (0.5 wt%), mainly to illustrate the large difference in behavior between the dilute situation and the semi-dilute/concentrated systems that are the subjects of this study. At 0.5 wt%, all systems form micelles and no significant intermolecular interactions between the micelles seem to appear in the form of correlation peaks. At higher concentrations, the scattering profiles for F127 and PCL(5) show correlation peaks for the higher two concentrations and the position of the maximum is shifted to a higher q-value with increasing polymer concentration. A decrease of the intermicellar distance with increasing concentration is expected because the number of micelles should increase, and this should yield a smaller average distance between the micelles. In the case of PCL(11), it was only possible to dissolve the polymer up to a concentration of 10 wt% due to high hydrophobicity; the corresponding scattering profile is not displaying any distinct correlation peak, suggesting a more disordered system. In addition, the strong upturn of the scattering curve at low q-values is a harbinger of large aggregates that is consistent with the high complex viscosity values (see Fig. 2).

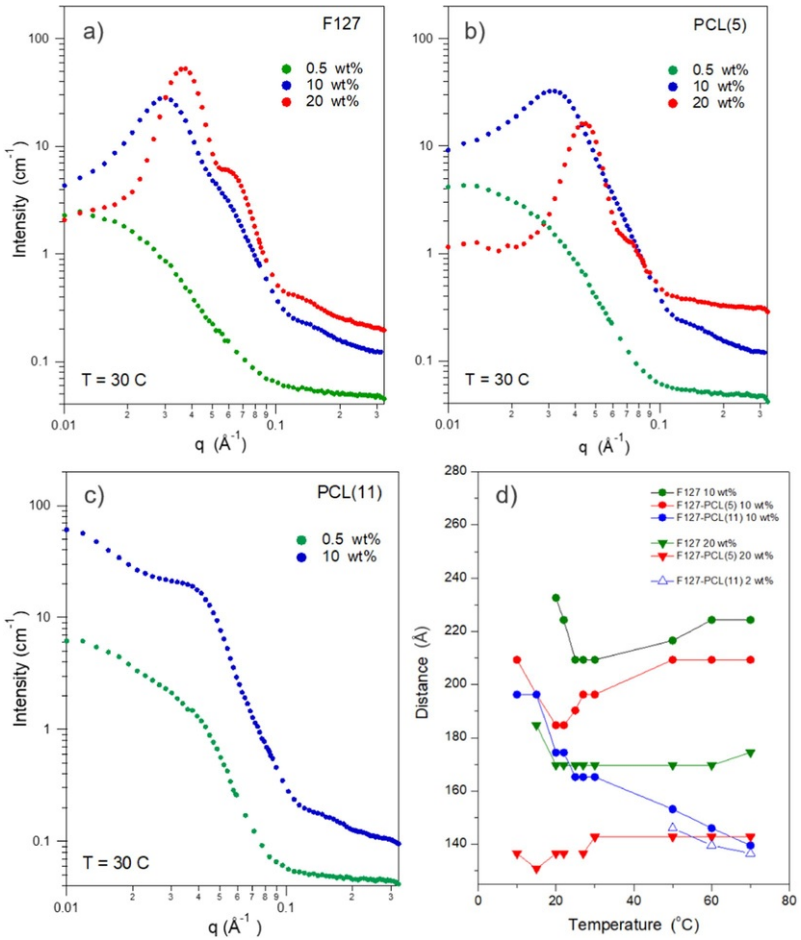

Fig. 7 SANS patterns at a fixed temperature (30 °C) for F127 (a), PCL(5) (b), and PCL(11) (c) at the concentrations indicated. d) Plot of the average intermicellar distance $d = 2\pi/q_{max}$ versus temperature for the systems indicated.

An inspection of the scattering profiles for F127 (Fig. 7a) discloses, especially at the highest polymer concentration (20 wt%), a main correlation speak is located at $q = 0.040\ Å^{-1}$ and a higher order Bragg interference peak, or rather a shoulder, is centered at $q = 0.069\ Å^{-1}$; this corresponds to a ratio of 1:1.73 (or $1:3^{1/3}$) that is an indication of cubic packing of the micelles [13,46,47]. However, a shoulder or a second order peak is also expected at $0.0565\ Å^{-1}$ ($1:2^{1/2}$), but as has been pointed out [13,46,47] the second order peak may be smeared with the first-order peak and they are too close to be resolved in SANS. It is possible to discern a broad shoulder on the scattering curve at higher q-value, centered at about $0.13\ Å^{-1}$, which can be ascribed to intraparticle interference [47]. For the 20 wt% PCL(5) sample at 30 °C (Fig. 7b), a distinct correlation peak is located at $0.045\ Å^{-1}$ and a broad shoulder centered at approximately $0.070\ Å^{-1}$; this yields a ratio of 1:1.56, which is somewhat lower than observed for F127. This may signalize a less ordered gel structure. For the PCL(11) at 10 wt% and a temperature of 30 °C (a gel is formed at these conditions) (Fig. 7c), only a weak interparticle peak is found and no higher order diffraction peaks appear indicating the absence of supramicellar structures [13,47]. It seems that the connected PCL-blocks abolish the ordered gel structure detected for F127.

The polymer concentration and temperature dependences of the average intermicellar distance $d = 2\pi/q_{max}$ for F127, PCL(5), and PCL(11) are illustrated in Fig. 7d. The general trend for F127 and PCL(5) is that at a fixed temperature (over the whole interval), the value of d drops when the concentration increases, whereas for PCL(11) the trend is reversed. The former inclination for the two other systems is easy to justify, because a higher polymer concentration should generate more micelles and hence the average intermicellar distance should decrease. The latter tendency is more intricate to explain, but it is possible that the PCL(11) sample of the highest concentration (10 wt%) forms intermicellar aggregates at elevated temperatures, whereas the 2 wt% solution exhibits incipient intermicellar interference first at ca. 50 °C and no signs of aggregation is detected over the considered temperature

domain. However, for the 10 wt% sample a strong upturn of the scattered intensity was found at low q already at 30 °C (Fig. 7c). This is an indicator of large aggregates and this irregularity can lead to a larger average intermicellar distance in the system (see also the discussion below about aggregation numbers). The observation for the F127 system that the value of d falls off when the polymer concentration increases, is consistent with some of the previous small angle scattering studies [13,25,46,47] on the F127 system, but it has also been argued that the impact of polymer concentration is small [12].

As is evident from Fig. 7d, the intermicellar distance for the copolymer systems depends also on the temperature. Let us first discuss the effect of temperature on the F127 samples. At 10 wt% (no temperature-induced gel is formed at this concentration), the value of d drops initially; this indicates that a temperature rise favors the creation of more micelles as a result of enhanced sticking probability of the unimers. After the minimum, the average distance is found to increase with increasing temperature; this trend suggests that more polymer chains are incorporated into each micelle, thereby reducing the number density of micelles and increasing the aggregation number. A reason for this behavior may be a change in the micelle equilibrium due to the strong dehydration of EO and PO segments at high temperatures. We can estimate the aggregation number N_{agg} from [48] $N_{agg} = c \cdot N_A \cdot d^3/M_w$, where c is the volume concentration (kg/m^3), N_A is the Avogadro constant, d is the intermicellar distance, and M_w weight average molecular weight. The results indicate that for F127 at 10 wt%, N_{agg} increases from 44 to 54 in the temperature interval 25–70 °C. The aggregation number estimated at 25 °C is in agreement with those reported previously [13,25]. At 10 wt% of PCL(5), a very similar temperature profile of d as that of F127 is detected, but in this case the average distance is significant shorter for this system than for pure F127 (Fig. 7d). This demonstrates that there are more micelles per volume unit for PCL(5), indicating that the aggregation number is also smaller for PCL(5) than for pure F127 micelles (given that the samples have the same concentration). For instance, at 70 °C, $N_{agg} = 35$ for PCL(5) in comparison with 54 for F127. This effect is expected since PCL(5) is more hydrophobic and it forms micelles at lower temperatures than F127 (cf. Fig. 5) and less number of unimers in the micelle is needed for its stabilization, leading to a larger number density of micelles.

For F127 at a polymer concentration of 20 wt% (an incipient gel is formed at ca. 13 °C), d falls off initially and some more micelles are formed at low temperatures, whereas above 20 °C the value of d is virtually constant and only a small increase of d is observed at the highest temperature; probably due to a heterogeneity in the gel-network when the macroscopic phase separation is approached (Fig. 7d). When the connectivity in the network has been established we do not expect the intermicellar distance to vary much under the condition that no major structural changes in the network takes place or macroscopic phase separation comes into play. For PCL(5) at 20 wt%, the initial small drop of d probably announces a higher number density of micelles before the incipient gel is formed and at temperatures from 15 °C up to 30 °C, d seems to increase in the network-forming process and at higher temperatures (30–70 °C) d is practically constant. In a previous SANS study on F127 in a buffer at a concentration of 21.2% (w/v) it was reported [46] that the position of the correlation peak was virtually independent of temperature in the range 25–50 °C; this is consistent with our results at 20 wt%. In another SANS investigation [47] on F127 at a concentration of 15%, they observed that the position of the intermicellar correlation peak was shifted to slightly lower q-values with increasing temperature in the interval (22–80 °C), that is, the value of d rises. This is compatible the present finding for the 10 wt% sample (cf. Fig. 7d).

A more complex and different behavior is observed for 10 wt% of the PCL(11) system. This sample forms an incipient gel at 21 °C and from the start (10 °C) to the gel point the aggregation number decreases from 25 to 17, suggesting that the number of polymer chains in each micelle is reduced and gradually more micelles are created, leading to smaller intermicellar distance. In the post-gel region, the value of d falls off over the whole considered temperature domain. If the aggregation number is calculated at the highest temperature (70 °C), a value of $N_{agg} = 9$ is obtained; this indicates a huge number of micelles with only a few polymer chains inside. Since the PCL end groups are fairly long for this copolymer it is possible that it forms flower-like micelles before the gel-point and when the gel-network is evolved it is likely that there are bridges connecting the micelles in the network. This may be the reason for the monotonous decrease of d in the post-gel region. However, we should also bear in mind that the SANS results for PCL(11) (cf. Fig. 6a) revealed the existence of aggregates outside the SANS-window and this may also contribute to the findings in ~~in~~ the post-gel regime for this strongly hydrophobic copolymer. In the case of the low concentration sample (2 wt%) of PCL(11), a correlation peak is only developed for the higher three temperatures and the trend is the same as for the high concentration sample, but the values of the intermicellar distance are lower (the aggregation numbers are smaller) (Fig. 7d) because fewer polymer chains are inside the micelles. This is again an illustration of that both polymer concentration and temperature govern the creation of micelles and intermicellar interaction.

To obtain a more quantitative picture of the SANS results we have conducted model fitting of the results at some conditions where the difference between the three polymers is particularly notable, and this is illustrated in Fig. 8. By employing a core-shell micelle model [49] with hard-sphere interaction between the micelles [25], the SANS data for 20 wt% F127 at 70 °C can be described very well (see Fig. 8a). It is found that the radius of the core is 67 Å and that of the shell 37 Å; the core radius is similar as reported previously for F127 [12]. It is interesting to note that still at this high temperature, the core contains a substantial amount of water. For a water-free core, containing only PPO-blocks, the scattering length density (SDL) value is expected to be $0.34 \cdot 10^{-6}$ Å^{-2}, but the fitted SLD-value is found to be significantly higher ($2.4 \cdot 10^{-6}$ Å^{-2}). Since the SLD-value for the solvent D_2O is $6.36 \cdot 10^{-6}$ Å^{-2}, this shows that the average water content is as high as 34% even at 70 °C. When it comes to the shell, we expect the water content to be high and the fitted SLD-value of $3.6 \cdot 10^{-6}$ Å^{-2} indicates an average water content of 52% for the shell, taking into account that the SLD for PEO alone is $0.572 \cdot 10^{-6}$ Å^{-2}. For 10 wt% of PCL(5) at 60 °C no conspicuous correlation peak is detected (Fig. 8b), but we should recall that a well-developed correlation peak is observed at lower temperatures and at all temperatures for the 20 wt% sample (see Fig. 5). This suggests that the spatial correlation between neighboring micelles is repressed. It should be noted that the core-radius is only approximately 30 Å compared to 68 Å for F127. This may be ascribed to a much lower aggregation number for PCL(5) in comparison with F127 ($N_{agg} = 35$ for PCL(5) in comparison with 54 for F127).

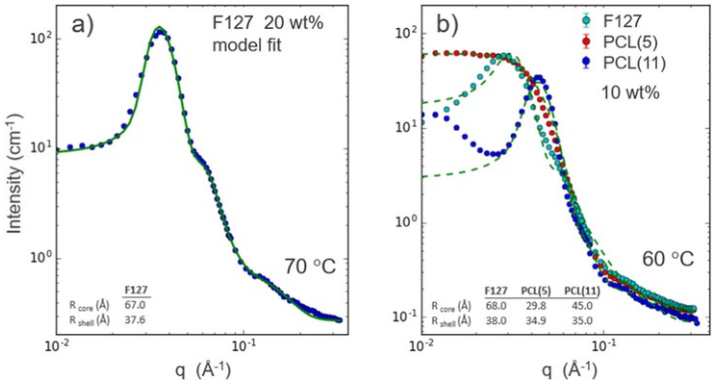

Fig 8 (a) SANS pattern of F127 (20 wt%) at 70 °C including model fitting using a core-shell model with hard-sphere interaction. (b) SANS patterns of F127 as well as the two modified samples (10 wt%) at 60 °C with model fitting. Note that the excess scattering at low q for PCL(11) i not fitted with the model. The fitted values for the radius of the core (R_{core}) and shell (R_{shell}) have been included as insets in (a) and (b).

In the case of PCL(11), there is a marked excess scattering at low q that cannot be fitted with the present model. This feature is probably related to the formation of large intermicellar structures. Actually, this excess scattering is visible already at low temperatures for PCL(11); a slope approaching −1 is observed in a log-log plot at low q at 25 °C (cf. Fig. 6b) and this is an indication of the creation of asymmetric structures. This may occur if the micelles tend to arrange into clusters containing a small number of micelles. Since the intermicellar distance is short and the aggregation number is low (ca. 17) this may readily take place.

4 Conclusions

In this work, we have studied temperature-induced intermicellar association and gelation of semidilute and concentrated aqueous solutions of the PEO-PPO-PEO triblock copolymer F127 and its hydrophobically modified analogs with short (PCL(5)) and long (PCL(11)) blocks at both ends of the chain. The results clearly show that phase behavior, gelation, rheology, and mesoscopic structure features are significantly affected by the incorporation of PCL-blocks. The phase behavior is similar for F127 and PCL(5) over an extended concentration and temperature interval and no turbidity is observed for F127, whereas turbidity is noticed for PCL(5) at high temperatures. At 25 wt%, the samples form gels at about 13–14 °C. It is not possible, due to its high hydrophobicity, to dissolve PCL(11) in water at concentrations above ca. 10 wt%. For this copolymer, turbidity is visible at fairly low temperatures and concentrations, and a gel is formed at about 21 °C for a 10 wt% sample.

The absolute complex viscosity |η*| values for 10 wt% of PCL(11) are more than two decades higher than for the two other copolymers and this is attributed to the high hydrophobicity of PCL(11) and its ability to form bridges between neighboring micelles. The frequency dependence of |η*| ($|\eta^*| \propto \omega^{-m}$) reveals that hard gels are formed in the post-gel region with $m \approx 0.9$ (approaching solid-like response). An interesting complex viscosity anomaly is clearly observed for disrupted networks of F127 at high frequencies, followed by kinetic arrest or jamming of the species and an increase in |η*|. This effect is a novel finding for Pluronic. In the case of PCL(11) the anomaly is more pronounced prior to the gel formation, and here the bridging of neighboring micelles may contribute to the magnitude of this effect.

The SANS results revealed that when the polymer concentration is high (10 and 20 wt%) unimers are only formed for F127 if the temperature was sufficiently low. At higher temperatures, a conspicuous correlation peak, indicative of interacting micelles, appeared at intermediate q-values. This peak discloses vital intermicellar correlations, and possible crystalline-like order. The position and width of the correlation peak were found to depend on polymer concentration, temperature, and hydrophobicity of the copolymer. In most cases, the scattering function could be described by using a spherical core-shell micelle model with hard sphere interaction between them. At some conditions, the correlation peak was found to be suppressed or disappeared and this may indicate that the micellar order is lost. This feature was observed for 10 wt% of PCL(5) at high temperatures and for 10 wt% of PCL(11) at intermediate temperatures (in the beginning of the gel region).

From the position of the maximum of the correlation peak, the intermicellar distance could be determined ($d = 2\pi/q_{max}$) and it was possible to estimate the aggregation number N_{agg}, which was found to depend on polymer concentration and temperature. Prominent differences were disclosed between the systems and the impact of the PCL groups on the self-assembling of the micelles and the intermicellar associations were fundamental. This study has clearly demonstrated that pronounced alterations in rheological and structural properties take place when Pluronic is modified with hydrophobic PCL groups.

Acknowledgements

This work was supported by the People Program (Marie CurieActions) of the European Union's Seventh Framework Program FP7/2007-2013/ under REA grant agreement no. 290251.

Appendix A. Supplementary material

Supplementary data to this article can be found online at https://doi.org/10.1016/j.eurpolymj.2019.01.033.

References

[1] G.S. Kwon and K. Kataoka, Block copolymer micelles as long circulating drug vehicles, *Adv. Drug Delivery Rev.* **16**, 1995, 295–309.

[2] Y. Kakizawa and K. Kataoka, Block copolymer micelles for delivery of gene and related compounds, *Adv. Drug Delivery Rev.* **54**, 2002, 203–222.

[3] A.V. Kabanov, P. Lemieux, S. Vinogradova and V. Alakhovb, Pluronic block copolymers: novel functional molecules for gene therapy, *Adv. Drug Delivery Rev.* **54**, 2002, 223–233.

[4] A. Agarwal, R. Unfer and S.K. Mallapragada, Novel cationic pentablock copolymers as non-viral vectors for gene therapy, *J. Control. Release* **103**, 2005, 245–258.

[5] M. Lazzari, G. Liu and S. Lecommandoux, Block copolymers in nanoscience, 2007, John Wiley & Sons.

[6] E.V. Batrakova and A.V. Kabanov, Pluronic block copolymers: evolution of drug delivery concept from inert nanocarriers to biological response modifiers, *J. Control. Release* **130**, 2008, 98–106.

[7] T. Schnitzler and A. Herrmann, DNA block copolymers: functional materials for nanoscience and biomedicine, *Acc. Chem. Res.* **45**, 2012, 1419–1430.

[8] M.T. Calejo, A.M.S. Cardoso, A.-L. Kjøniksen, K. Zhu, C.M. Morais, S.A. Sande, A.L. Cardoso, M.C.P. de Lima, A. Jurado and B. Nyström, Temperature-responsive cationic block copolymers as nanocarriers for gene delivery, *Int. J. Pharm.* **448**, 2013, 105–114.

[9] H. Hu, M. Gopinadhan and C.O. Osuji, Directed self-assembly of block copolymers: a tutorial review of strategies for enabling nanotechnology with soft matter, *Soft Matter* **10**, 2014, 3867–3889.

[10] B. Claro, K. Zhu, S. Bagherifam, S.G. Silva, G. Griffiths, K.D. Knudsen, E.F. Marques and B. Nyström, Phase behavior, microstructure and cytotoxicity in mixtures of a charged triblock copolymer and an ionic surfactant, *Eur. Polym. J.* **75**, 2016, 461–473.

[11] P. Alexandridis, F. Holzwarth and T.A. Hatton, Micellization of poly(ethylene oxide)-poly(propylene oxide)-poly(ethylene oxide) triblock copolymers in aqueous solutions: Thermodynamics of copolymer association, *Macromolecules* **27**, 1994, 2414–2425.

[12] K. Mortensen and Y. Talmon, Cryo-TEM and SANS microstructural study of Pluronic polymer solutions, *Macromolecules* **28**, 1995, 8829–8834.

[13] R.K. Prud'homme, G. Wu and D.K. Schneider, Structure and rheology studies of poly(oxyethylene−oxypropylene−oxyethylene) aqueous solution, *Langmuir* **12**, 1996, 4651–4659.

[14] M. Bohorquez, C. Koch, T. Trygstad and N. Pandit, A study of the temperature-dependent micellization of pluronic F127, *J. Colloid Interface Sci.* **216**, 1999, 34–40.

[15] C.C. Fraenza, C. Mattea, G.D. Farrher, A. Ordikhani-Seyedlar, S. Stapf and E. Anoardo, Rouse dynamics in PEO-PPO-PEO block-copolymers in aqueous solution as observed through fast field-cycling NMR relaxometry, *Polymer* **150**, 2018, 244–253.

[16] M.J. Park and K. Char, Gelation of PEO−PLGA−PEO triblock copolymers induced by macroscopic phase separation, *Langmuir* **20**, 2004, 2456–2465.

[17] L. Yu and J. Ding, Injectable hydrogels as unique biomedical materials, *Chem. Soc. Rev.* **37**, 2008, 1473–1481.

[18] N. Gjerde, K. Zhu, B. Nyström and K.D. Knudsen, Effect of PCL end-groups on the self-assembling process of Pluronic in aqueous media, *Phys. Chem. Chem. Phys.* **20**, 2018, 2585–2596.

[19] S. Tanodekaew, J. Godward, F. Heatley and C. Booth, Gelation of aqueous solutions of diblock copolymers of ethylene oxide and d, l-lactide, *Macromol. Chem. Phys.* **198**, 1997, 3385–3395.

[20] R.G. Larson, The Structure and Rheology of Complex Fluids, 1999, Oxford University Press; New York.

[21] H.H. Winter, Evolution of rheology during chemical gelation, *Prog. Colloid Polym. Sci.* **75**, 1987, 104–110.

[22] M. Doucet et al. SasView Version 4.1.2, Zenodo, 10.5281/zenodo.825675.

[23] R.-J. Roe, Methods of X-Ray and Neutron Scattering in Polymer Science, 2000, Oxford University Press; New York.

[24] K. Mortensen and J. Skov Pedersen, Structural study on the micelle formation of poly(ethylene oxide)-poly(propylene oxide)-poly(ethylene oxide) triblock copolymer in aqueous solution, *Macromolecules* **26**, 1993, 805–812.

[25] B. Cabane, K. Lindell, S. Engström and B. Lindman, Microphase separation in polymer + surfactant systems, *Macromolecules* **29**, 1996, 3188–3197.

[26] N.S. Othman, M.S. Jaafar, A.A. Rahman, E.S. Othman and A.A. Rozlan, Ultrasound speed of polymer gel mimicked human soft tissue within three weeks, *Int. J. Biosci. Bioinf.* **1**, 2011, 223–225.

[27] G. Wanaka, H. Hoffmann and W. Ulbricht, The aggregation behavior of poly-(oxy.ethylene)-poly-(oxypropylene)-poly-(oxyethylene)-block-copolymers in aqueous solution, *Colloid Polym. Sci.* **268**, 1990, 101–117.

[28] G.-E. Yu, Y. Deng, S. Dalton, Q.-G. Wang, D. Attwood, C. Price and C. Booth, Micellisation and gelation of triblock copoly(oxyethylene/oxypropylene/oxyethylene), F127, *J. Chem. Soc., Faraday Trans.* **88**, 1992, 2537–2544.

[29] M. Malmsten and B. Lindman, Self-assembly in aqueous block copolymer solutions, *Macromolecules* **25**, 1992, 5440–5445.

[30] F. Tanaka and W.H. Stockmayer, Thermoreversible gelation with junctions of variable multiplicity, *Macromolecules* **27**, 1994, 3943–3954.

[31] F. Tanaka and M. Ishida, Elastically effective chains in transient gels with multiple junctions, *Macromolecules* **29**, 1996, 7571–7580.

[32] A.N. Semenov and M. Rubinstein, Thermoreversible gelation in solutions of associative polymers. 1. Statics, *Macromolecules* **31**, 1998, 1373–1385.

[33] G. Wanka, H. Hoffmann and W. Ulbricht, Phase diagrams and aggregation behavior of poly(oxyethylene)-poly(oxypropylene)-poly(oxyethylene) triblock copolymers in aqueous solutions, *Macromolecules* **27**, 1994, 4145–4159.

[34] K. Hyun, J.G. Nam, M. Wilhellm, K.H. Ahn and S.J. Lee, Large amplitude oscillatory shear behavior of PEO-PPO-PEO triblock copolymer solutions, *Rheol Acta* **45**, 2006, 239–249.

[35] C.R. López-Barrón, L. Porcar, A.P.R. Eberle and N.J. Wagner, Dynamics of melting and recrystallization in a polymeric micellar crystal subjected to large amplitude oscillatory shear flow, *Phys. Rev. Lett.* **108**, 2012, 258301-1–258301-5.

[36] H.H. Winter and F. Chambon, Analysis of linear viscoelasticity of a crosslinking polymer at the gel point, *J. Rheol.* **30**, 1986, 367–382.

[37] E. Zaccarelli, Colloidal gels: equilibrium and nonequilibrium routes, *J. Phys. Condens. Matter.* **19**, 2007, 323101.

[38] K.N. Nordstrom, E. Verneuil, P.E. Arratia, A. Basu, Z. Zhang, A.G. Yodh, J.P. Gollub and D.J. Durian, Microfluidic rheology of soft colloids above and below jamming, *Phys. Rev. Lett.* **105**, 2010, 175701–175704.

[39] A. Basu, Y. Xu, T. Still, P.E. Arratia, Z. Zhang, K.N. Nordstrom, J.M. Rieser, J.P. Gollub, D.J. Duriana and A.G. Yodh, Rheology of soft colloids across the onset of rigidity: scaling behavior, thermal, and non-thermal responses, *Soft Matter* **10**, 2014, 3027–3035.

[40] Y.H. Wen, J.L. Schaefer and L.A. Archer, Dynamics and rheology of soft colloidal glasses, *ACS Macro Lett.* **4**, 2015, 119–123.

[41] J.M. Bricker and J.E. Butler, Oscillatory shear of suspensions of noncolloidal particles, *J. Rheol.* **50**, 2006, 711–728.

[42] Y. Lin, N. Phan-Thien and B.C. Khoo, Short-term and long-term irreversibility in particle suspensions undergoing small and large amplitude oscillatory stress, *J. Rheol.* **57**, 2013, 1325–1346.

[43] C.R. López-Barrón, N.J. Wagner and L. Porcar, Layering, melting, and recrystallization of a close-packed micellar crystal under steady and large-amplitude oscillatory shear flows, *J. Rheol.* **59**, 2015, 793–820.

[44] N.K. Khorshid, K. Zhu, K.D. Knudsen, S. Bekhradnia, S.A. Sande and B. Nyström, Novel structural changes during temperature-induced self-assembling and gelation of PLGA-PEG-PLGA triblock copolymer in aqueous solutions, *Macromol. Biosci.* **16**, 2016, 1838–1852.

[45] J.E. Nielsen, K. Zhu, S.A. Sande, L. Kovácik, D. Cmarko, K.D. Knudsen and B. Nyström, Structural and rheological properties of temperature-responsive amphiphilic triblock copolymers in aqueous media, *J. Phys. Chem.* **121**, 2017, 4885–4899.

[46] C. Wu, T. Liu, B. Chu, D.K. Schneider and V. Graziano, Characterization of the PEO-PPO-PEO triblock copolymer and its application as a separation medium in capillary Electrophoresis, *Macromolecules* **30**, 1997, 4574–4583.

[47] Y. Li, T. Shi, Z. Sun, L. An and Q. Huang, Investigation of sol-gel transition in Pluronic F127/D2O solutions using a combination of small-angle neutron scattering and Monte Carlo simulation, *J. Phys. Chem. B* **110**, 2006, 26424–26429.

[48] T. Koga, F. Tanaka, R. Motokawa, S. Koizumi and F.M. Winnik, Theoretical modeling of associated structures in aqueous solutions of hydrophobically modified telechelic PNIPAM based on a neutron scattering study, *Macromolecules* **41**, 2008, 9413–9422.

[49] J.S. Pedersen and M.C. Gerstenberg, Scattering form factor of block copolymer micelles, *Macromolecules* **29**, 1996, 1363–1365.

Appendix A. Supplementary material

The following are the Supplementary data to this article:

Multimedia Component 1

Supplementary Data 1

Graphical abstract

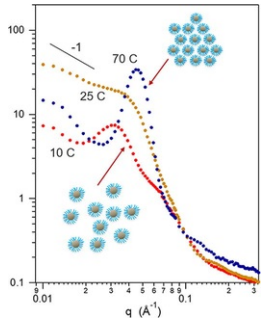

Highlights

- The viscosity and gelation of Pluronic are significantly affected by PCL end-groups.
- An interesting complex viscosity anomaly is observed for the systems.
- The position of the correlation peak from SANS is dependent on temperature and concentration.

Queries and Answers

Query: Your article is registered as a regular item and is being processed for inclusion in a regular issue of the journal. If this is NOT correct and your article belongs to a Special Issue/Collection please contact v.g@elsevier.com immediately prior to returning your corrections.